PAGEOPH, Vol. 144, Nos. 3/4 (1995) 0033-4553/95/040855-20$1.50 + 0.20/0

The 1994 Shikotan Earthquake Tsunamis

HARRY YEH,[1] VASILY TITOV,[2] VIACHESLAV GUSIAKOV,[3] EFIM PELINOVSKY,[4] VASILY KHRAMUSHIN,[5] and VICTOR KAISTRENKO[5]

Abstract—The 1994 Shikotan earthquake was one of the greatest earthquakes in recent years with a magnitude of M_s 8.0. A tsunami survey was conducted by Russian and U.S. geophysicists from October 16–30, 1994, less than two weeks after the earthquake. The survey results and a numerical hindcast simulation are reported. Tsunami focusing effect at locations supposedly sheltered by the island chain is discussed. Based on the obtained data, tsunamis which attacked Shikotan Island are characterized as long waves (the order of 10–20 min wave period) with a positive leading wave. Possible consequences of the positive leading wave form are discussed in relation to the observed minimal destruction of beach vegetation and relatively small transport of marine sediment onto the shore. The high-quality tide-gage record in Malokurilskaya Bay indicates the occurrence of a 53 cm subsidence at the site.

Key words: Earthquake, tsunamis, runup, South Kuril Islands, numerical simulation, tide gage, subsidence.

Introduction

On October 4, 1994, at 13:23 p.m. GMT, an earthquake of magnitude M_s 8.0 (based on Obninsk Seismic Center, Russia) struck the southern region of the Kuril Islands. On Shikotan Island, one of the South Kuril Islands, located closest to the earthquake epicenter, ground shaking was extremely intense: the intensity was reported to be between 9 and 10 on the Modified Mercalli Intensity Scale. An approximately 1.8 m tsunami runup in Nemuro, Japan, was reported approximately 90 minutes after the earthquake (SATAKE, 1994) and Pacific-wide tsunami warnings were issued, including the coastal regions of Hawaii and the west coasts of the United States and Canada. In the South Kuril Islands, 11 people were killed and 242 were injured. In Hokkaido, Japan, one person was killed and 140 were injured.

[1] Department of Civil Engineering, University of Washington, Seattle, Washington 98195, U.S.A.
[2] University of Southern California, Los Angeles, California, U.S.A.
[3] Computer Center, Novosibirsk, Russia.
[4] Institute Applied Physics, Nizhny Novgorod, Russia.
[5] Institute of Marine Geology and Geophysics, Yuzhno-Sakhalinsk, Russia.

None of the casualties were due directly to the tsunami in spite of its significant runup (approximately 10 m high runup on Shikotan Island). The total casualty toll was light for a magnitude M_s 8.0 earthquake. Perhaps this is because the earthquake occurred in the middle of the night (0:23 a.m. Oct. 5, local time) when people were sleeping in their houses; most of the residential houses were made of wood which tends to be invulnerable to shaking. On the other hand, inadequately reinforced masonry structures, commonly used as daytime working places, could not withstand the strong shaking and were destroyed. There was no fire caused by this earthquake; the climate was mild so that heating systems were not in use and the village-wide centralized and well-controlled heating and electric systems helped prevent igniting fire from domestic locations. More importantly, the South Kuril areas have experienced many large earthquakes and tsunamis (see Table 1), hence the people were well prepared for this natural disaster.

Remarkable effects of the earthquake to note were the formations of many large gaping fissures and landslides evidently due to very strong ground shaking. For example, near Malokurilsk, Shikotan, major fissure formations were observed on the grass covered hill: the main fissure is a maximum of 60 m wide and approximately 350 m long; one end of the fissure leads to the approximatley 80 m high shore precipice (see Fig. 1). Because of the strong ground shaking, the earthquake also generated significant secondary environmental impacts due especially to leakage of oil from many oil storage tanks.

Table 1

The tsunamigenic earthquakes occurred in the area within 42.0–46.0°N and 145.0° – 150.0°E. The data listed are limited to those with the tsunami intensity, I, greater than 0: the tsunami intensity I is based on SOLOVIEV *(1972). The data were compiled based on* SOLOVIEV *(1978) and* SOLOVIEV *et al. (1986).*

Year	Date	Latitude (N)	Longitude (E)	Depth (km)	Magnitude (M_s)	I	Max. tsunami runup height (m)
1843	4/25	44.70	149.70	40	8.2	2.5	4.50
1893	6/03	43.10	147.00	40	6.6	1.0	1.50
1894	3/22	42.50	145.10	40	7.9	2.0	4.00
1958	11/06	44.53	148.54	40	8.2	2.5	5.00
1958	11/12	44.39	148.70	40	7.4	0.0	1.00
1961	2/12	43.88	147.65	50	7.0	0.0	1.00
1963	10/13	44.80	149.50	47	8.1	2.5	5.00
1963	10/20	44.80	150.20	60	7.4	3.0	15.00
1969	8/11	43.58	147.82	40	8.2	2.0	5.00
1973	6/17	43.15	145.88	55	7.9	1.0	1.50
1973	6/24	43.38	146.52	57	7.4	0.0	1.20
1975	6/10	43.20	147.50	30	7.1	2.0	5.50
1978	3/23	43.70	149.30	40	7.6	1.5	0.17
1978	3/23	43.90	148.30	40	7.8	0.0	0.26
1978	3/24	43.90	149.10	30	7.9	0.0	0.65
1994	10/04	43.84	147.59	33	8.0	2.5	9.00

Figure 1
Major fissure formations near Malokurilsk, Shikotan. The fissure, maximum 60 m wide, 15 m deep, and approximately 350 m long, is formed parallel to the major landslide (approximately 80 m high) along a shoreline precipice. Note that the size of trees shown left of the fissure is approximately 8 m high and the white spots that appear on the lower hill next to the precipice are full-size cows.

From October 16 through 30, 1994, the tsunami reconnaissance survey was conducted by fifteen Russian scientists and two members from the United States. Results of the survey and geophysical aspects of this earthquake are reported in this paper.

Seismological Background and Earthquake Mechanism

This earthquake occurred in one of the most seismically active areas of the Kuril-Kamchatka region. There were at least 27 recorded tsunamigenic earthquakes in the area between 42.0–46.0°N and 145.0°–150.0°E. Significant ones with tsunami intensity (based on SOLOVIEV, 1972) greater than 0 are listed in Table 1.

The earliest and probably the largest event occurred on April 25, 1843 (magnitude $M_s = 8.2$). The exact position of epicenter for this event is unknown but severe seismic shaking and damage were reported in the large area between Urup Island in the north and Kushiro, Japan, in the south. The data on tsunami heights on the South Kurils are not available, but IIDA (1984) reported 4.5 m waves near Kushiro. The next large event in the area occurred on March 22, 1894 ($M_s = 7.9$) with a

reported maximum tsunami runup of 4 m at Miyako, Japan. After this event there had been no large (with $M_s > 7.9$) earthquake until 64 years later on November 6, 1958 when an earthquake of $M_s = 8.2$ occurred near Iturup Island. This earthquake generated tsunamis and the maximum runup height of about 5 m was reported on the east coast of Iturup Island. In 1963, a couple of large earthquakes struck successively within a week at virtually the same location near Urup Island. Another large earthquake (on August 11, 1969; $M_s = 8.2$) struck the same region, about 1.5 degrees SW of the 1958 event and 3.5 degree SW of the 1963 events. The maximum runup height which reached 5 m was measured on the east coast of Shikotan Island. The aftershock areas of both the 1958 and 1969 events, based on the seismological observations, overlap by at least 50 km along the trench direction (HATORI, 1990).

The present Shikotan earthquake of October 4, 1994, occurred at the same location as the 1969 event. The aftershock clouds of both events almost coincided; the deviation in the cloud locations was only in the order of 20–30 km. Other recent and substantial earthquakes occurred at the same location. At the NE edge of the 1994 Shikotan earthquake source, and earthquake of $M_s = 7.1$ occurred on June 10, 1975. Despite its magnitude, tsunamis with 5.5 m height were measured at the nearest coast. The 1975 event is considered to be an example of a so-called tsunami earthquake (KANAMORI, 1972; FUKAO, 1979; KANAMORI and KIKUCHI, 1993). Furthermore, the SW edge of the 1994 Shikotan earthquake source is also overlapped with the source area of the June 17, 1973 earthquake ($M_s = 7.9$). Figure 2 shows the recent significant earthquakes which occurred in the South Kuril area. The numerous significant earthquakes in the same area in such a short time interval contradicts the framework of the seismic-gap theory which suggests that a large

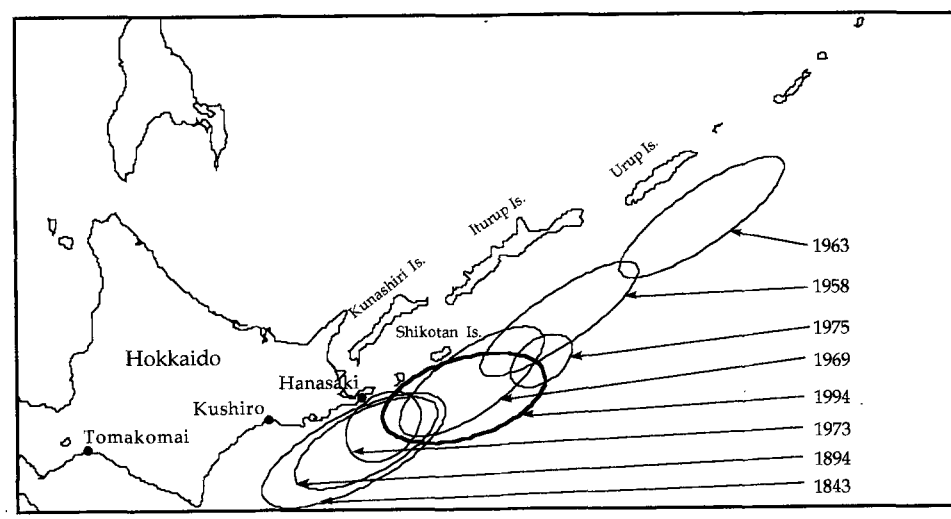

Figure 2
Distribution of source areas of some historical South Kuril tsunamis.

subduction earthquake tends to occur in a seismically quiet region adjacent to a seismically active neighborhood, for example, the Shumagin seismic gap along the Aleutian trench (JACOB, 1984).

The aftershock distribution shown in Figure 3 indicates that the seismic activities associated with the earthquake occurred at the continental slope. Harvard University's centroid moment tensor determination for the 1994 Shikotan earthquake was obtained about 6 hours after the main shock. The best double-couple solution consists of two planes, none of which can be considered to represent the low-angle thrust typical of the subduction region. The first plane dips at an angle 40° to the SW and strikes almost perpendicular to the trench axis. The second plane with strike direction 52°, which is roughly parallel to the trench axis, dips 77° to the SE so that its predominant source mechanism should be the reverse dip-slip fault with a considerable (slip angle 128°) strike component. This uncertainty with regard to source mechanism hopefully will be resolved later on the basis of detailed seismological investigation.

Note that this area is poorly covered by the regional seismic networks. To demonstrate the degree of accuracy in source parameter estimates, eight different main shock positions, determined by different seismological agencies, are listed in Table 2 and are presented in Figure 3. The widely scattered main shock locations exceed one degree in both latitude and longitude coordinates. Based on the seismological data available, it appears that the source mechanism of the 1994

Table 2

The main shock information determined by different agencies: the estimated locations of the main shock are also plotted on Figure 3

Latitude	Longitude	Time of of occurrence	Depth	Magnitude (M_s)	Agency
43.40 N	147.60 E	13:23		7.8	YS
43.68 N	147.63 E	13:22:57	33 km	8.0	OBN
43.22 N	147.40 E	13:23	30 km	8.1	JMA
43.39 N	147.08 E	13:23:05	46 km	8.1	HOKK
43.661 N	147.335E	13:22:58.1	33 km	8.1	NEIC
43.67	147.36 E	13:23:25	64 km	8.3	HARV
43.90 N	147.20 E	13:23	33 km	8.2	PTWC
43.80 N	148.60 E	13:23	33 km	8.1	ATWC

YS: Yuzhno-Sakhalinsk Seismic Station, Russia
OBN: Obninsk Seismic Center, Russia
JMA: Japan Meterological Agency, Japan
HOKK: the Research Center for Earthquake Prediction at Hokkaido University, Japan
NEIC: National Earthquake Information Center, USA
HARV: Harvard University, USA
PTWC: Pacific Tsunami Warning Center, USA
ATWC: Alaska Tsunami Warning Center, USA

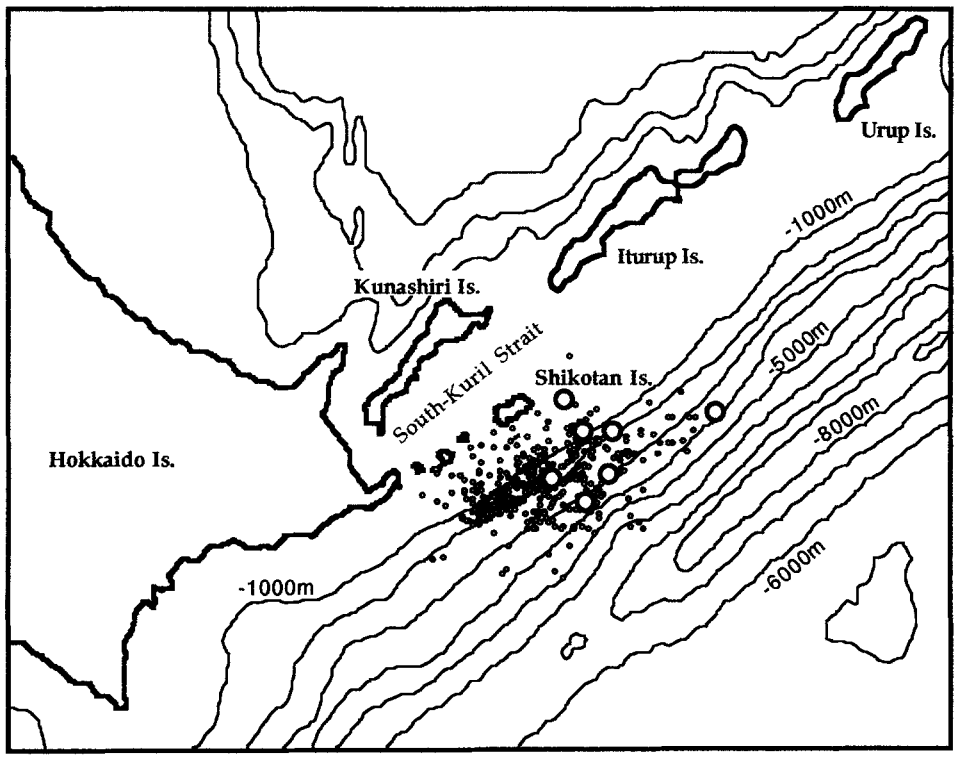

Figure 3
Bathymetry contours, and one-week-aftershock distribution, o, and several different estimates of epicenter locations, O, for the October 4, 1994 Shikotan earthquake. (The aftershock data are provided by the Research Center for Earthquake Prediction of Hokkaido University.)

Shikotan earthquake contained a complex nature in which several major planes ruptured during the event and several large crustal blocks displaced (possibly in different directions).

Tsunami Runup Distributions

A tsunami source condition was estimated based on the best-fit double-couple of the Harvard University centroid moment tensor solution and seismic moment 2.1×10^{28} dynes-cm. Estimating the source area to be 120×100 km based on the aftershock distribution (Fig. 3), with the consideration of an approximately 50 cm subsidence at Shikotan Island (as discussed later), an initial water-surface displacement was determined as shown in Figure 4. Based on this initial condition, the numerical simulation was carried out. The numerical model is a finite-difference scheme, based on the fully nonlinear shallow-water wave equation in the characteristic

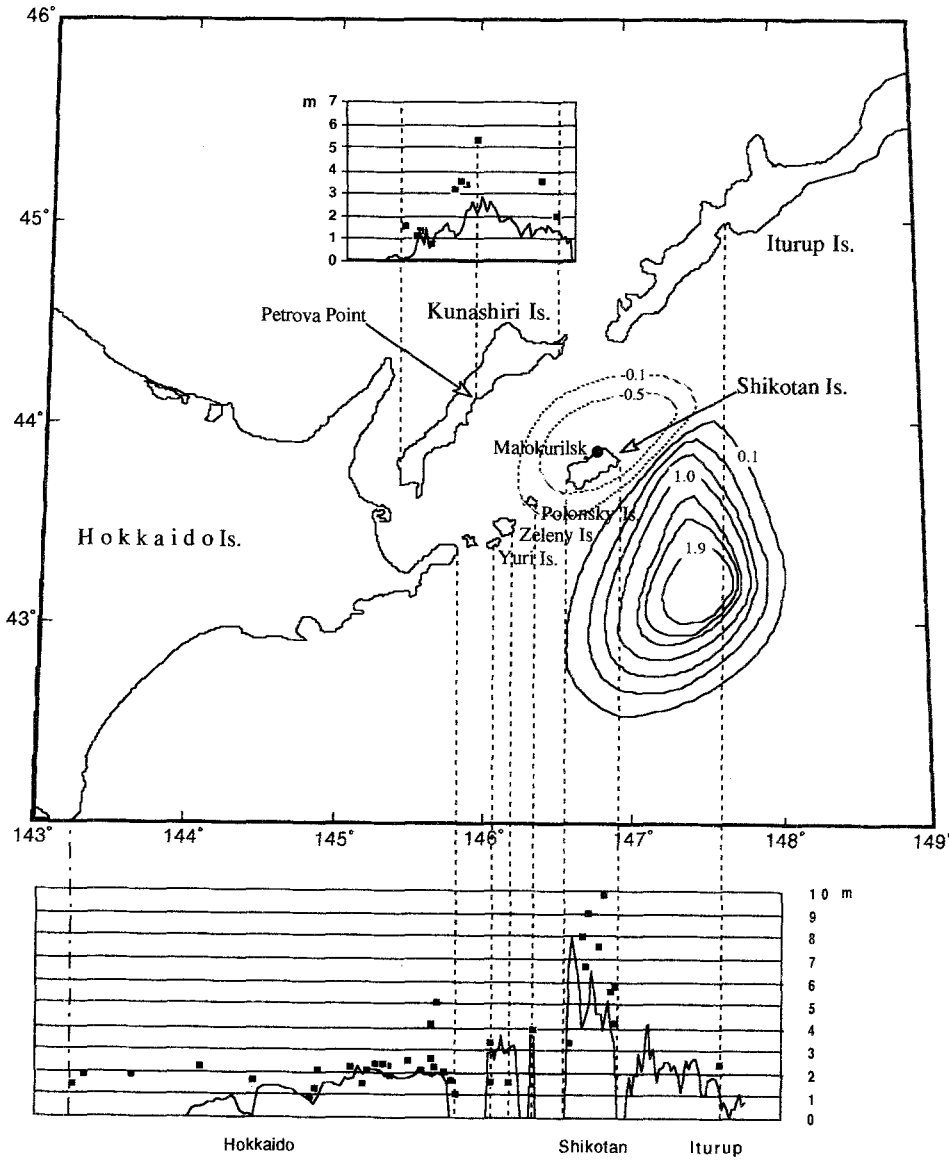

Figure 4

Initial sea-level displacement (in meters) used for the numerical model and tsunami runup heights from sea level at the time of the tsunami attack: ——, the numerical simulation model; ■, measured highest values of each location. All the runup values are those on the south-east side of the islands, i.e., facing to the tsunami source.

form (TITOV and SYNOLAKIS, 1993): the spatial grid sizes used are 4 km in deep water (depth greater than 300 m) and 0.9 km in shallow water (depth less than 300 m), and the computational time step used is 6 seconds. As pointed out earlier, the mechanism of this earthquake is complex and not fully understood at this point: it appears that this was not a simple subduction earthquake but, at least during the initial stage, the plate was buckled perpendicular to the subduction line. Consequently, it is difficult to determine an accurate estimate of the initial sea-bottom deformation; the results presented in Figure 4 (shown with our field data as discussed later) should be considered as initial attempts for the simulation. It is anticipated that more refinements and corrections for the simulations will be performed.

Tsunami runup height measurements were made in Shikotan, Iturup, Kunashiri and small islands between Shikotan and Hokkaido (e.g., Polonsky, Zeleny, and Yury Islands). Numerous measurements along the Hokkaido coast were carried out by the Tohoku University group in Japan (TAKAHASHI and SHUTO, 1994). The measurements were made using similar procedures as in other recent surveys (e.g., SATAKE *et al.*, 1993, in Nicaragua; Yeh *et al.*, 1993, in Flores Island; HOKKAIDO TSUNAMI SURVEY GROUP, 1993, in Okushiri Island and CHOI *et al.*, 1994, in Korea). No global positioning system (GPS) was used in our survey except on Shikotan Island. Considering that detailed maps and charts in the region were available, the lack of GPS caused no inconvenience nor did we lose any important information in our survey results. The compiled data are shown in Figure 4, together with the numerical simulation results. Note that the measured data were corrected to values of the vertical runup heights from sea level at the time of tsunami attack. In spite of the complexity of the rupture mechanism of this earthquake, the comparisons of the numerical predictions and measurements are in good agreement. Note that this degree of agreement between the measured and simulated runup values was not achieved in the cases of the 1992 Nicaragua, the 1992 Flores, the 1993 Okushiri, and the 1994 Java tsunamis. It is noted that the Nicaragua and Java tsunamis are considered to have been "tsunami" earthquakes (KANAMORI, 1972; FUKAO, 1979; KANAMORI and KIKUCHI, 1993), and the Flores and Okushiri tsunamis were caused by "backarc-thrust" earthquakes (PLAFKER and WARD, 1992), in which rupture patterns were very complex. Also there is considerable evidence for submarine landslides in Flores that might have enhanced the tsunami runup heights (PLAFKER, 1995).

The measured runup data shown in Figure 4 indicate that there is a locally high (5.3 m) runup location near Petrova Point, approximately 13 km north-east of Yuzhno-Kurilsk, on Kunashiri Island; the numerical simulation also exhibits a local maximum at the same location (see Fig. 4). Based on the assumed tsunami generation region, Kunashiri Island is located behind the Shikotan-Polonsky-Zeleny-Yury Islands chain, hence the tsunami propagation to Kunashiri Island must have been partially blocked by the island chain. As shown in Figure 5, the primary

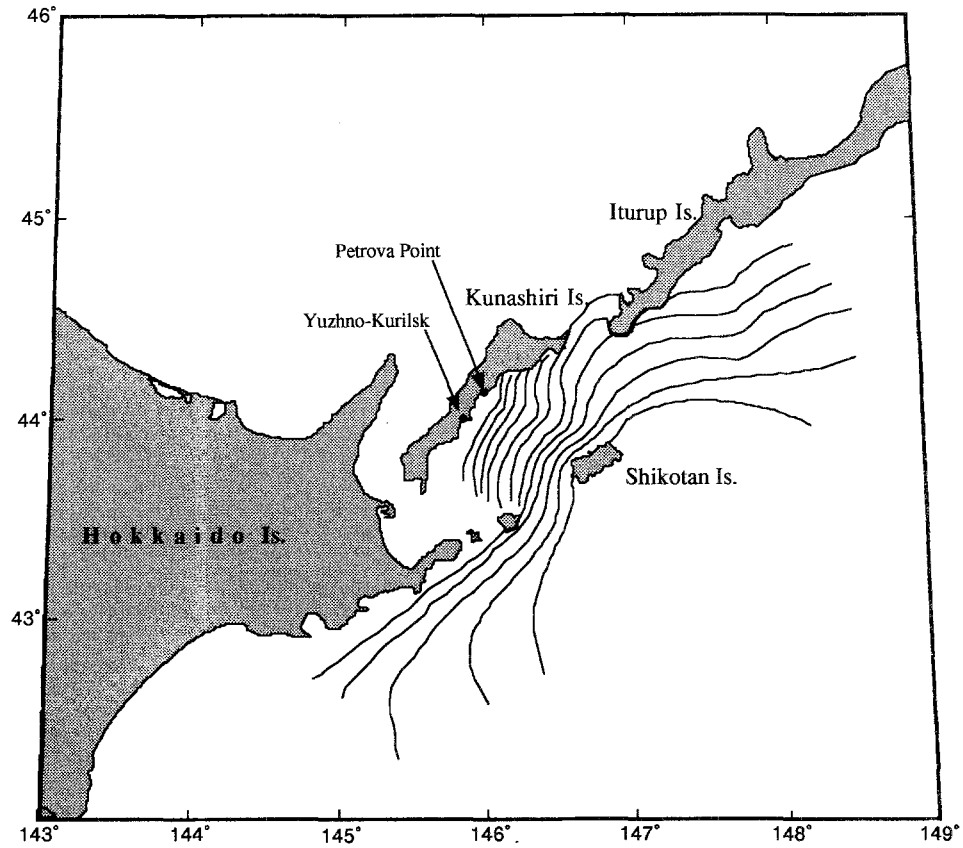

Figure 5
A sequence of the numerically simulated leading tsunami crests with the time intervals of 5 minutes. The tsunami focusing effect near Petrova Point is evident.

tsunami path to reach Kunashiri Island was through the mouth of the South Kuril Strait, between Shikotan and Iturup Islands (see Fig. 3 for the area of the South Kuril Strait). The water depth between Shikotan and Iturup Islands is deeper (approximately 200 m) than the depth (approximately 50 m) of the South-Kuril Strait, between Shikotan and Kunashiri Islands. The gap between Shikotan and Polonsky Islands (Fig. 4) is approximately 20 km wide and 40 m deep and some of the tsunami energy from the Pacific Ocean could have passed through. All other gaps are considered to be too shallow (less than 10 m deep) for substantial tsunami energy to penetrate into the South-Kuril Strait from the Pacific. Our explanation for the large runup height near Petrova Point on Kunashiri Island is as follows. The deeper channel along the mouth of the South-Kuril Strait caused tsunami refraction to guide the propagation westward into the South-Kuril Strait, i.e., directing the tsunami propagation to the middle of Kunashiri Island towards Petrova Point.

Meanwhile, small-but-sufficient tsunami energy which passed through the gap between Shikotan and Polonsky Islands reached Petrova Point; this tsunami met the previously mentioned tsunami that had traveled around the east side of Shikotan Island from the mouth of the South-Kuril Strait. The superposition of two waves caused higher runup near Petrova Point than those measured at other locations. Such effects are qualitatively verified in the numerical simulation model as demonstrated in Figure 5: similar effects were shown in the computer animation independently performed by TAKAHASHI and SHUTO (1994). As will be discussed later with Figure. 9, the water depth of the South-Kuril Strait is shallow (approximately 50 m) and the bottom slope is very mild (approximately 0.1 degree slope), hence submarine landslides are unlikely to occur near Petrova Point.

Runup Distribution Around Shikotan Island

On Shikotan Island, measurements were made at 85 different locations around the island. Note that approximatley 80% of the island's coastline is a series of nearly vertical cliffs and not readily accessible. Except in very few cases (one or two), measurements were made based on very conservative and strict tsunami runup marks, i.e., only marine-origin objects were considered to be appropriate for tsunami runup marks. The measured runup heights around the island are plotted in Figure 6. Note that the values presented in the figure are not all individual measurements but are the local maximum values. As a typical survey example, individual measurements made at Tserkovnaya Bay are presented in Figure 7.

Figures 6 and 7 show that the magnitudes of runup are fairly uniform: the average runup height is 6.1 m on the south side of the island with a standard deviation of 1.8 m, while on the north side of the island, the average runup height is 2.5 m with a standard deviation of 0.2 m. The higher runup heights on the south side of the island confirm that the primary tsunamis must have attacked from the south, and north side of the island was in the shadow zone for this tsunami event. The substantial difference in runup height also suggests that the order of magnitude of tsunami wavelength must have been comparable or smaller than the island dimension; if the tsunami wavelength had been much longer than the island dimension, then the runup heights would have been uniform all around the island, just like tides being uniform around the island. On the other hand, if the tsunami wavelengths were shorter than the length scale of local features (e.g., bays, coves, headlands, and small islands), then the runup distribution along the southern coast of the island would have been substantially affected by the local features: instead, we found the measured runup heights to be fairly uniform along the coast as shown in Figures 6 and 7, indicating that the tsunami wave length must have been long enough. The dimension of Shikotan Island is at the order of 15 km and the order of magnitude of the depth of the sea surrounding the island is approximately 50 m.

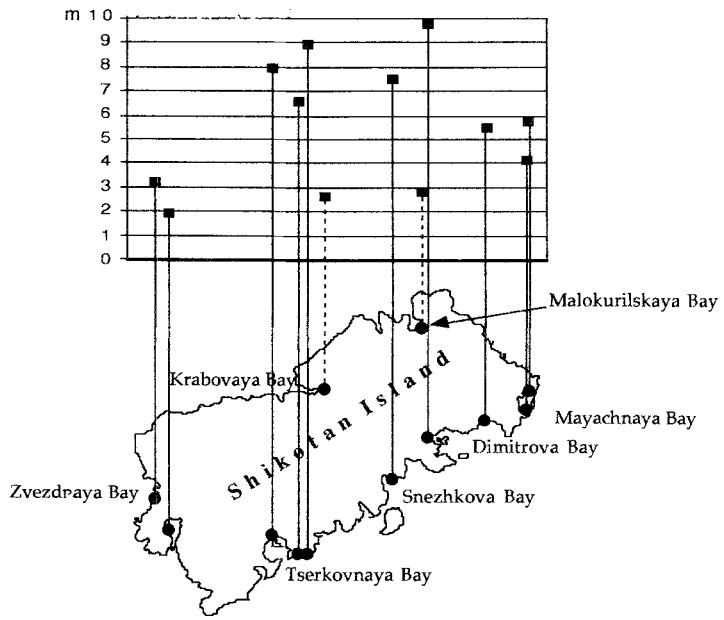

Figure 6
Tsunami runup heights around Shikotan Island. The values are from sea level at the time of the tsunami attack (we assume that the 53 cm island subsidence (see Fig. 11) occurred prior to the tsunami attack).

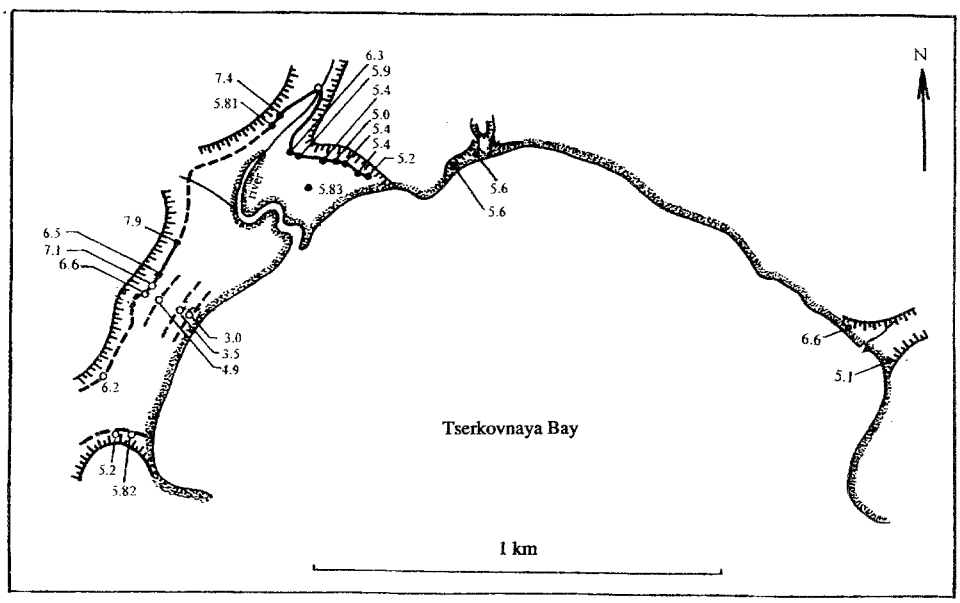

Figure 7
Individual runup measurements (vertical runup heights in meter from sea level at the time of the tsunami attack) at Tserkovnaya Bay.

If a half tsunami wave length is shorter than the island dimension and approximating the propagation speed by that of the shallow-water waves, i.e., a square root of the product of depth and gravity acceleration, then the tsunami wave period must have been less than 23 minutes. The dimensions of local features of the southern coast is at the order of 3 km in horizontal and 30 m in depth, thus the tsunami wave period must have exceeded 6 minutes. Therefore, we estimate the tsunami period to be between 6 and 23 minutes. This estimated range of tsunami period concurs with the numerical simulation result, approximately 20 minutes of the initial tsunami oscillation period. An additional explanation for the difference in runup height between the south and north sides of the island must be related to the shape of the island. As seen in Figure 6, Shikotan Island has a rectangular shape, which is not a shape favorable for waves to propagate around the shadow zone of the island. Most of the tsunami energy propagating along the east and west sides cannot be diffracted into the north side due to the sharp curvature of the shoreline at the north-east and north-west corners of the island.

At Tserkovnaya Bay, we found at least four different tsunami runup marks (3.0, 3.5, 4.9 and 7.1 m) along a transact perpendicular to the shoreline as shown in Figure 7. This means that there were at least four tsunamis attacked at the south coast of Shikotan. Another noteworthy observation from our survey in Shikotan was the fact that we could find no excessive sediment sheet formations nor noticeable transports of beach rocks on the tsunami runup areas. Furthermore, beach grass, bushes, and trees are still intact, although there are many clear signs of tsunami inundation. For example, one of the tsunami traces found at Tserkovnaya Bay is the marine-origin seaweed which clung to a tree branch as shown in Figure 8 which also shows the good vegetation conditions in the tsunami runup areas. It is well-known that tsunamis are capable of transporting substantial sediments onto the runup areas from offshore (ATWATER, 1987; BOURGEOIS *et al.*, 1988; DAWSON *et al.*, 1988; MINOURA and NAKAYA, 1991). Excessive sediment layers and transport of beach rocks and corals were found in the previous surveys of the 1992 Nicaragua tsunamis and the 1992 Flores tsunamis, as well as in the 1993 Okushiri tsunamis survey. Note that the runup heights, approximately 6 m high, measured on the south shore of Shikotan are comparable to the runup heights measured in Nicaragua and Flores, and the south-side Shikotan beaches are sandy beaches, at least near the shoreline. The lack of transported sediments and beach rocks, and the good vegetation conditions on the runup areas evidently suggest that the runup motion on Shikotan must be different from the other tsunami cases; the runup on Shikotan must have been a gradual process. This conjecture is consistent with the fact that the measured runup heights are fairly uniform regardless of the different local topography. Additional explanations could be related to the indication of the inital wave being positive. As discussed later, both tide-gage recordings in Malokurilskaya Bay, Shikotan, and Hanasaki Harbor, Hokkaido, show that the initial tsunami formation was a positive wave. In comparison to the case of an

Figure 8
A tsunami trace found at Tserkovnaya Bay, see the seaweed clinging in the shrub.

initial negative wave followed by a positive wave, the initial positive wave tends to cause smaller runup heights and less violent runup motions; these effects were first demonstrated by GOLUBTSOVA and MAZOVA (1989) and MAZOVA (1991) and the theory was refined by TADEPALLI and SYNOLAKIS (1994). Perhaps, those are the factors which minimized destruction of vegetation, scattering beach rocks, and the formation of sand layers.

Even though approximately 80% of the Shikotan coastal line was not accessible for the survey, regarding surveyed areas, no abnormally high runup region was found: the order of magnitudes of all the measured runup heights can be explained by the numerical simulations. As mentioned earlier, this was not the case for the past several tsunamis; for example, the maximum runup of 26 m measured in Riangkroko (in Flores, Indonesia) could not be explained until evidence of massive nearshore submarine landslides was discovered (PLAFKER, 1995). In spite of several massive landslides observed at many places on Shikotan Island, the occurrence of underwater landslides is very unlikely near Shikotan Island. Figures 9a, b and c display an evident contrast in bathymetry between Shikotan, Okushiri (Japan), and Flores (Indonesia) Islands. The bathymetry of both Okushiri and Flores Islands is very steep around the islands, while in spite of the very ragged terrain above the sea level, the sea bottom is uniform and shallow in the sea surrounding Shikotan Island. Hence, significant submarine landslides are not possible. Incidentally, the

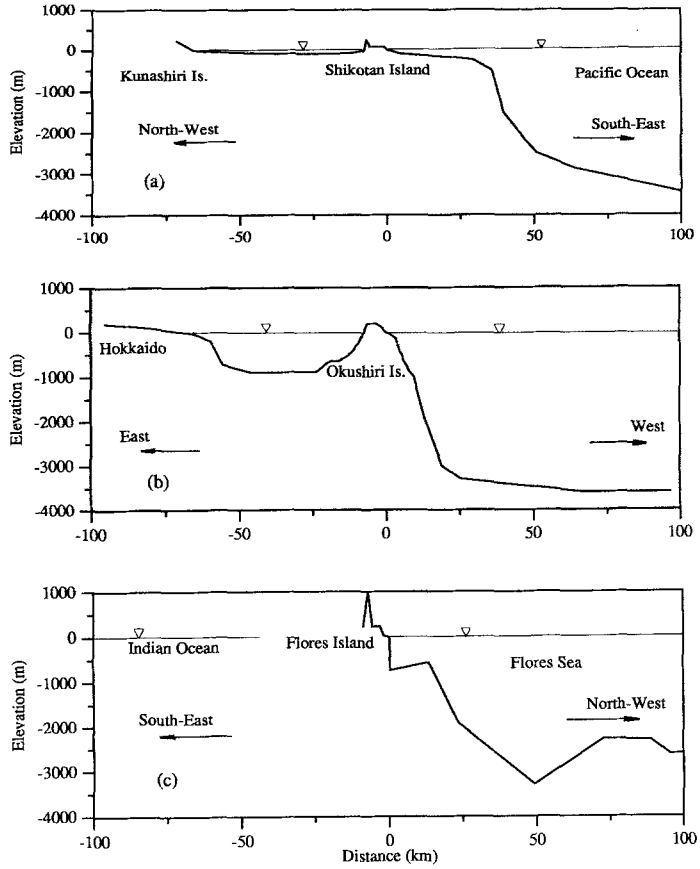

Figure 9
Comparison of sea bottom profiles: a) Shikotan, b) Okushiri Island, and c) Flores Island: the origin is set at the island shoreline.

shallow uniform sea bottom in the South-Kuril Strait (see Fig. 3) resulted in substantial sedimentary deposits with the maximum sediment thickness of more than 4,000 meters (SNEGOVSKOY *et al.*, 1987).

Tide Gage Data at Malokurilskaya Bay

This tsunami event left quality tide-gage records at Malokurilskaya Bay in Shikotan, Hanasaki Harbor in Hokkaido, Poronaisk in Sakhalin, and among others in Japan. The tide gage record at Hanasaki Harbor (see Fig. 2 for its location) shows that the first wave was a positive wave with the wave oscillation periods of 30 minutes (see Fig. 10a). Other than the tide gages, the ultrasonic wave gage placed in 18.5 m deep offshore of Tomakomai Port, Hokkaido (see Fig. 2 for

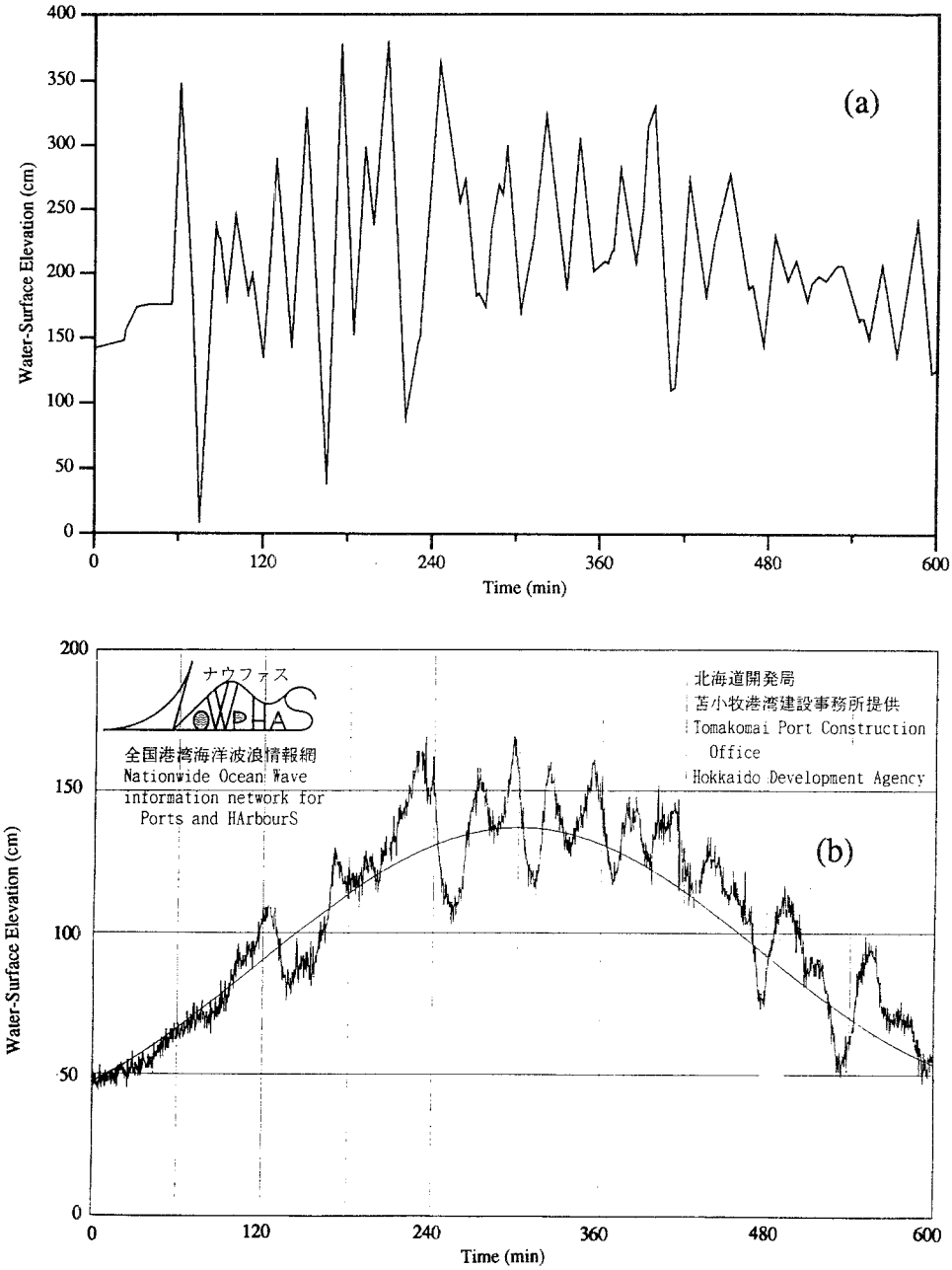

Figure 10
Tsunami measurements in Hokkaido, Japan. a) The tide-gage record in Hanasaki Harbor (the original analog data taken by the Japan Meteorological Agency were digitized and processed); b) Tsunami profile recorded by an ultrasonic wave gage (18.5 m deep) off Tomakomai (after NAGAI *et al.*, 1995). The time origin corresponds to 0:00 a.m. the South-Kuril local time and the earthquake occurred at 0:23 a.m. See Figure 2 for the locations.

its location), captured the tsunami record as shown in Figure 10b. This record was numerically low-pass-filtered because high wind-wave conditions with more than 2 m significant wave heights were present at the time of the measurements. The record reveals that the tsunami arrival time was approximately 1:35 a.m. Kuril local time (14:35 p.m. GMT, that is 1 hour after the earthquake). Just like the record at Hanasaki Harbor (Fig. 10a), the first wave at Tomakomai was a positive wave, and the tsunami periods were very long, in the order of 50 minutes (NAGAI *et al.*, 1995). In this paper, we will focus on the data taken in Malokurilskaya Bay, Shikotan, only 70 km away from the epicenter and closest to the tsunami generation area.

Figure 11a illustrates the tide gage record in the Malokurilskaya Bay (the original analog record was digitized and processed to eliminate the tracer-ink smudge presumably caused by the strong shake). The bay has nearly a circular shape (approximately 800 m in diameter) with the narrow entrance (approximately 350 m wide). The well maintained tide gage is located at the east shore of the bay with a well diameter of 65 cm. The Malokurilskaya Bay is known to have a distinct Helmholtz oscillation period of 18.5 minutes (GJUMAGALIEV and RABINOVICH, 1993), and Figure 11a evidently shows the contamination of the tsunami record due to this Helmholtz oscillation. According to the record shown in Figure 11a, the arrival time of the first tsunami peak was approximately 40 minutes after the main shock; it also took 40 minutes for the tsunami crest to arrive at Hanasaki Harbor (Fig. 10a). It is noted that our numerical model shows that the first-peak arrival time is 30 minutes after the earthquake. The data after removing astronomical tides are presented in Figure 11b which also displays the evident mean water-level shift of 53 cm after the earthquake. The data presented in Figure 11b are considered to be a rare quantitative recording of the land subsidence with the tide gage. According to Figure 11a, the initial rise of water level appears to take place immediately after the main shock and was a slow process: at Hanasaki (Fig. 10a), the initial rise was much faster than that shown in Figure 11a. This gradual rise of the water level could have been created by filling water in the subsided region from the surrounding area, rather than the main tsunamis generated off the Pacific Ocean.

Daily averaged tidal levels were computed from the tide gage records by GUSEVA *et al.* (1994). The data were further adjusted by eliminating the daily variations caused by astronomical tides, and the results are presented in Figure 11c. Note that the data presented in the figure is based on GMT, hence the value of the October 4 record represents the average of pre-earthquake sea level for 13.5 hours and the post-earthquake sea level for 10.5 hours. As shown in Figure 11b, the actual subsidence took place in much shorter duration (less than one hour). This evidently shows that the major subsidence of the island (53 cm) occurred at the main shock followed by the gradual subsidence of about 30 cm from Octover 9 to 13, 1994; note that there was a strong aftershock, M_s 7.4 on October 9. Subsequently, the daily averaged sea level appeared to decrease in the last two days of the

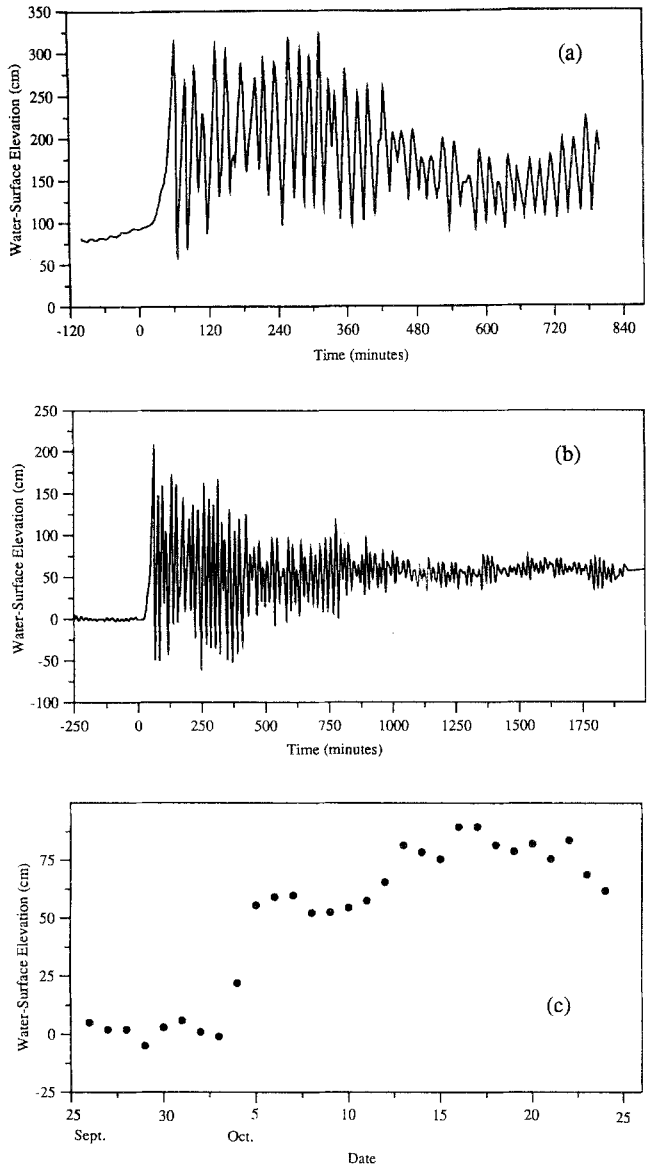

Figure 11

The tide-gage record in Malokurilskaya Bay: a) raw data after digitization (the tracer-ink smudge presumably caused by the strong shake, that appears on the original analog data, was eliminated in the digitization process): the time origin corresponds to 0:00 a.m. local time and the earthquake occurred at 0:23 a.m., b) after removal of the astronomical tides (the time origin is the same as that presented in a), and c) daily average data: the date is based on GMT.

data (October 23 and 24). Physical interpretations for this gradual increase and decrease of sea level are not clear at this time and no explanation is given here.

An eyewitness report in Malokurilskaya Bay indicates that the leading wave was a positive wave followed by approximately 2.5 m of negative wave, which is consistent with the tide gage data presented in Figure 11a. The resulting current was so swift that no ship could cross the bay entrance nor approach the shore for the first 2.5 hours, the current speed of approximately 6 m/sec was reported by an eyewitness. The bottom sounding showed that the water depth at the center of the bay changed from 5 m to 8 m, evidently due to tsunami scouring effects.

Summary

The 1994 Shikotan earthquake was undoubtedly one of the largest earthquakes in recent years. In this very seismically active region, in spite of uncertainty in the earthquake rupture mechanism, resulting tsunami effects were simulated reasonably with the numerical model based on the shallow-water wave theory.

Some noteworthy effects are that the tsunami runup was enhanced at the mid-south coast of Kunashiri Island: the location appears to be protected from the tsunami source because it is behind the Shikotan-Polonsky-Zeleny-Yury Islands chain. Tsunami refraction around the mouth of the South Kuril Strait and merging tsunamis which leaked from the gap between Shikotan and Polonsky Islands might be the expalantion for this large runup.

Based on the runup distribution around the island and the runup conditions, the leading tsunami form that attacked Shikotan Island appears to be a positive wave with a gradual water surface increase. Such leading wave characteristics are consistent with the tide gage data recorded in Malokurilskaya Bay. The positive and gradually rising leading wave might have resulted from the observed minimal destruction of beach vegetation and relatively small transport of marine sediment onto the shore. The tide gage recorded the subsidence of the gage site by 53 cm at the event of the earthquake.

In spite of the many significant landslides observed on Shikotan Island, any substantial underwater slumping was unlikely to occur because of the shallow and uniform sea bottom bathymetry. This is another reason why no abnormally high local tsunami runup was observed on Shikotan Island.

Acknowledgment

The analog tide gage data at Malokurilskaya Bay were digitized and processed by E. Novikova and the data at Hanasaki Harbor were digitized and processed by D. Akkeson. The survey team consisted of V. Djumagliev, S. Gusiakov, V.

Kaistrenko, A. Kharlamov, A. Klochkov, Y. Korolyov, A. Kruglyakov, E. Kulikov, V. Kurakin, B. Levin, E. Pelinovsky, A. Poplavsky, E. Shelting, V. Titov, H. Yeh, L. Zhukova and N. Zolotukhina. This international survey was arranged by A. Ivachenko. HY thanks the members of the Institute of Marine Geology and Geophysics, Sakhalin, and the Russian Army, Shikotan for their hospitality and friendship. The travel support for VT was made possible by a National Science Foundation grant funded to C. Synolakis. This survey was supported by the Russian Fund of Basic Research, the Presidium of the Far Eastern Division of the Russian Academy of Sciences and the US National Science Foundation.

REFERENCES

ATWATER, B. F. (1987), *Evidence for Great Holocene Earthquakes along the Outer Coast of Washington State*, Science *236*, 942–944.

BOURGEOIS, J., HANSEN, T. H., WIBERG, P., and KAUFFMAN, E. G. (1988), *A Tsunami Deposit at the Cretaceous-Tertiary Boundary in Texas*, Science *241*, 567–570.

CHOI, B. *et al.* (1994), *Tsunami Survey of East Coast of Korea due to the* 1993 *Southwest of the Hokkaido Earthquake*, J. Korean Soc. Coastal and Ocean Eng., *6*, 117–125.

DAWSON, A. G., LONG, D., and SMITH, D. E. (1988), *The Storegga Slides: Evidence from Eastern Scotland for a Possible Tsunami*, Marine Geology *82*, 271–276.

FUKAO, Y. (1979), *Tsunami Earthquakes and Subduction Process near Deep-sea Trenches*, J. Geoph. Res. *84*, 2303–2314.

GJUMAGALIEV, V. A., and RABINOVICH, A. B. (1993), *Long-wave Investigation at the Shelf and in the Bays of South Kuril Islands*, J. Korean Soc. Coastal and Ocean Eng. *5*, 318–328.

GOLUBSTOBA, T. C., and MAZOVA, R. Kh. (1989), *The runup of waves of sign-variable form.* In *Oscillation and Waves in Fluid Mechanics* (ed. Petrukhin, N. S.) (Gorky Polytechnical Institute Press, Gorky 1989) pp. 30–43 (Russian).

GUSEVA, T., GALAGANOV, O., YAKOVLEV, F., MISHIN, A., KOZHURIN, A., PHILIPOV, M., YANKUSH, A., and VASILENKO, N. (1994), *Results of the Geological Survey and Satellite Geodesic Measurements at Shikotan Island*, 18–30 October of 1994, Special Report 23–31 (Russian).

HATORI, T. (1990), *Behaviour of the Kuril Tsunamis at the Hokkado and Sakhalin Coast Facing the Okhotsk Sea*, Zisin *43*, 493–498.

HOKKAIDO TSUNAMI SURVEY GROUP (1993), *Tsunami Devastates Japanese Coastal Region*, EOS *74*, 417 and 432.

IIDA, K. (1984), *Catalog of Tsunamis in Japan and its Neighboring Countries*, Special Report, Aichi Institute of Technology, Japan, 52 pp.

JACOB, K. H. (1984), *Estimates of Long-term Probabilities for Future Great Earthquakes in the Aleutians*, Geophys. Res. Lett. *11*, 295–298.

KANAMORI, H. (1972), *Mechanism of Tsunami Earthquakes*, Phys. Earth Planet. Inter. *6*, 346–359.

KANAMORI, H., and KIKUCHI, M. (1993), *The 1992 Nicaragua Earthquake: A Slow Tsunami Earthquake Associated with Subducted Sediments*, Nature *361*, 714–716.

MAZOVA, R. Kh. (1991), *The runup description for monochromatic wave propagating from the deep water.* Presented at the International Workshop on Long Wave Runup, Catalina Island, Calif. (also In *Report on the International Workshop on Long-wave Runup*, by Liu, P., Synolakis, C., and Yeh, H., J. Fluid Mech. *229*, 675–688, 1991).

MINOURA, K., and NAKAYA, S. (1991), *Traces of Tsunami Preserved in Inter-tidal Lacustrine and Marsh Deposits: Some Examples from Northeast Japan*, J. Geology *99*, 265–287.

NAGAI, T., HASHIMOTO, N., SHIMIZU, K., and TAKAYAMA, T. (1995), *Tsunami profiles observed at the NOWPHAS offshore wave stations*, Second International Workshop on Wind and Earthquake Engineering for Offshore and Coastal Facilities, University of California, Berkeley, Calif.

PLAFKER, G., and WARD, S. N. (1992), *Backarc Thrust Faculting and Tectonic Uplift along the Caribbean Sea Coast During the April 22, 1991, Costa Rica Earthquake*, Tectonics *11*, 709.

PLAFKER, G. (1995), personal communication.

SATAKE, K. (1994), Communication through Tsunami Bulletin Board dated Oct 4/94.

SATAKE, K., BOURGEOIS, J., ABE, K., TSUJI, Y., IMAMURA, F., IIO, Y., KATAO, H., NOGUERA, E., and ESTRADA, F. (1993), *Tsunami Field Survey of the 1992 Nicaragua Earthquake*, EOS *74*, 145, 156–157.

SNEGOVSKOY, S. S., KRANSY, M. L., and SERGEYEV, K. F. *Thickness of sediment deposits.* In *Geology-Geophysics Atlas of the Kuril-Kamchatka Island System* (eds. Segeyev, K. F. and Kransy, M. L.) (Academy of Sciences of the USSR 1987).

SOLOVIEV, S. L., *Basic data on tsunamis on the Pacific coast of the USSR, 1737–1976.* In *Izuchenie tsunami v otkrytom okeane (Study of Tsunami in the Open Ocean)* (Moscow, Nauka Publishing House 1978) pp. 61–136 (in Russian).

SOLOVIEV, S. L., GO, Ch.N., and KIM, X. S. *Catalog of tsunamis in the Pacific Ocean, 1969–1982* (Moscow, Soviet Geophysical Committee 1986) 164 pp. (in Russian).

SOLOVIEV, S. L., *Earthquakes and tsunami recurrence in the Pacific ocean.* In *Volny Tsunami* (*Tsunami Waves*) (Proceeding of Sakh. Complex Res. Inst. 1972) 29, pp. 7–47 (in Russian).

TADEPALLI, S., and SYNOLAKIS, C. E. (1994), *The Run-up of N-waves on Sloping Beaches*, Proc. R. Soc. Lond. A. *445*, 99–112.

TAKAHASHI, T., and SHUTO, N. (1994), personal communication.

TITOV, V. V., and SYNOLAKIS, C. E. (1993), *A numerical study of wave runup of the September 1, 1992 Nicaraguan tsunami*, Proc. IEGG/IOC International Tsunami Symposium, Wakayama, Japan, 627–635.

YEH, H., IMAMURA, F., SYNOLAKIS, C., TSUJI, Y., LIU, P., and SHI, S. (1993), *The Flores Island Tsunamis*, EOS *74*, 369, 371–373.

Measured runup data are available upon request to HY.

(Received February 13, 1995, revised March 28, 1995, accepted April 8, 1995)